ACS APPLIED NANO MATERIALS

May 2, 2025
Volume 8
Number 17
pubs.acs.org/acsanm

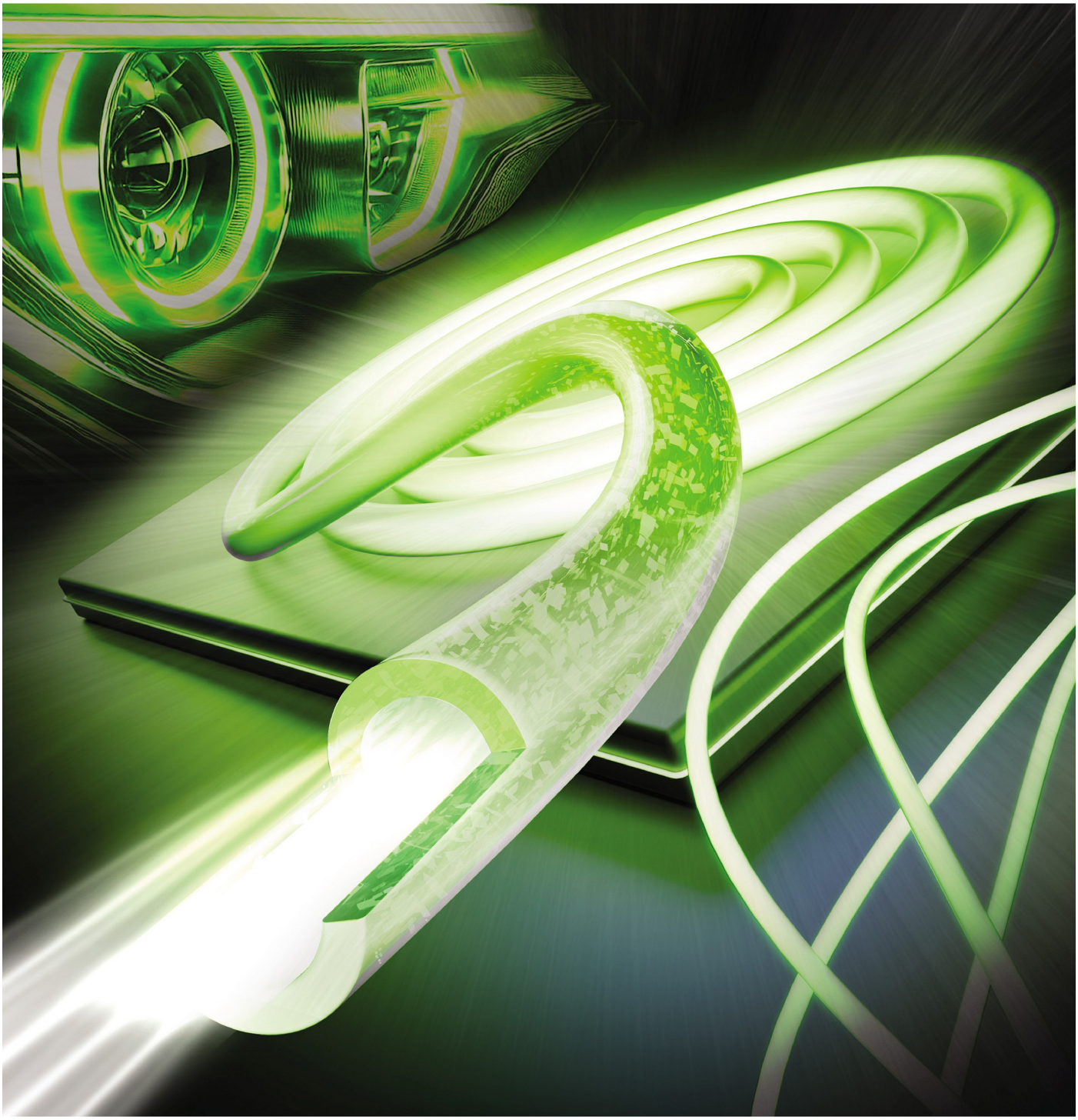

ACS Publications
Most Trusted. Most Cited. Most Read.

www.acs.org

ACS APPLIED NANO MATERIALS

www.acsanm.org

Article

Side-Emitting Optical Fibers of Colloidal Quantum Wells for Application in Curved-Surface Lighting and Sensing

Zahra Adelpour, Farzan Shabani, Mojtaba Sadeghi, Aisan Khaligh, Mahmudur Rahman, Fırat Karaboğa, Emre Ünal, Mustafa Ordu, and Hilmi Volkan Demir*

Cite This: ACS Appl. Nano Mater. 2025, 8, 8603−8611

Read Online

ACCESS | Metrics & More | Article Recommendations | Supporting Information

ABSTRACT: As specialized optical fibers, side-emitting optical fibers (SEOFs) are designed to emit light from their sides rather than their ends for possible applications in curved-surface lighting and sensing. In this study, we propose and demonstrate an in situ decoration of SEOFs with colloidal quantum wells (CQWs) for the first time. The proposed method enables the homogeneous distribution of CQWs in the polymeric matrix of the fiber with high side-emission efficiency, which is based on a simple yet effective method of CQW sheet coating. Two different structures of CQWs, a red-emitting CdSe/CdZnS core/shell and a green-emitting CdSe/CdS core/crown, were synthesized and employed in SEOFs. Accordingly, carefully tuned concentrations of CQWs were incorporated within the hollow-core optical fibers, and the side-scattered light from the fibers was systematically characterized and analyzed. The results confirm excellent side-emitting characteristics that are highly dependent on the optical fiber structure and CQW absorption spectrum. The average quantum yield values of 51 ± 5% and 34.5 ± 5% for different concentrations of red and green CQWs relative to their solution form were measured in our experiment, which is associated with polymeric medium, cluster formation, and fiber tower temperature. The findings pave the way for developing high-performance optical fiber devices based on CQW-doped SEOFs capable of efficient and precise light emission targeting a wide variety of applications ranging from three-dimensional curved-surface lighting to sensing.

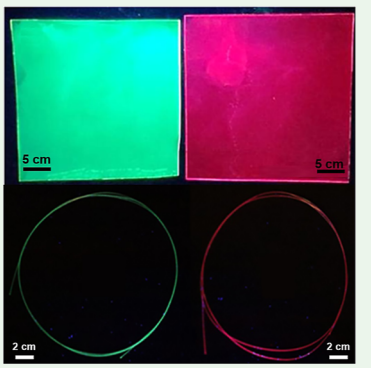

KEYWORDS: *side-emitting optical fibers, colloidal quantum wells, absorption, hollow-core optical fibers, polymeric matrix, light scattering*

INTRODUCTION

Light transmission, being totally confined in the core, is considered as the basic operational principle of optical fibers. In contrast to conventional usage, alternative applications of optical fibers can be introduced in which the desired operation is the scattering of light into the cladding and surrounding environment. This type of fibers, known as side-emitting optical fibers (SEOFs), finds usage in different application areas in the fields of medicine and healthcare monitoring,[1−3] sensing,[4,5] defense and security technologies,[6,7] and UV curing of resins and adhesives.[8,9] Moreover, these passive lighting structures can be used in textiles in a variety of different shapes and forms.[10] Such smart fabrics may also serve various functions of light harvesting, storage, and drug release and they may find use even in the fashion industry.[11,12]

To understand the side-emitting mechanism, it is helpful to refer to the well-known total internal reflection (TIR) phenomenon. When the incident angle is smaller than the critical angle ($\theta_{crit} = \sin^{-1}(n_{cladding}/n_{core})$), where $n_{cladding}$ and n_{core} are refractive indexes of the cladding and the core, respectively, the TIR condition is not satisfied and light leaks to the cladding. Nonguided modes are then coupled to radiation modes leading to the side emission. Thus, in SEOFs, the main goal is to reduce the incident angle below the critical angle to further facilitate the light leakage. To date, different approaches have been reported to achieve efficient side emitting of light in fibers. Among them are bending (with the bending radius close to or greater than the radius of the optical fiber),[13,14] bulk scattering (by adding particles in which the particles' density, shape, and refractive index result in side emission),[15] treatment of the fiber surface by sand blasting, mechanical pressure, or other forms of physical structuring[16] and adding luminescence particles (dopants that isotropically re-emit light at different frequencies).[17] Luminescent materials change the path of a light ray by isotropically re-emitting light that has previously been absorbed. These materials typically emit light through processes like fluorescence or phosphorescence, and their luminescent properties are due to their specific chemical composition. The emission wavelength of luminescent materials is often determined by their chemical composition, which can be tuned to some extent but may have

Received: December 3, 2024
Revised: February 20, 2025
Accepted: February 24, 2025
Published: March 4, 2025

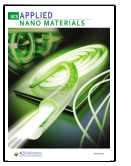

https://doi.org/10.1021/acsanm.4c06791
ACS Appl. Nano Mater. 2025, 8, 8603−8611

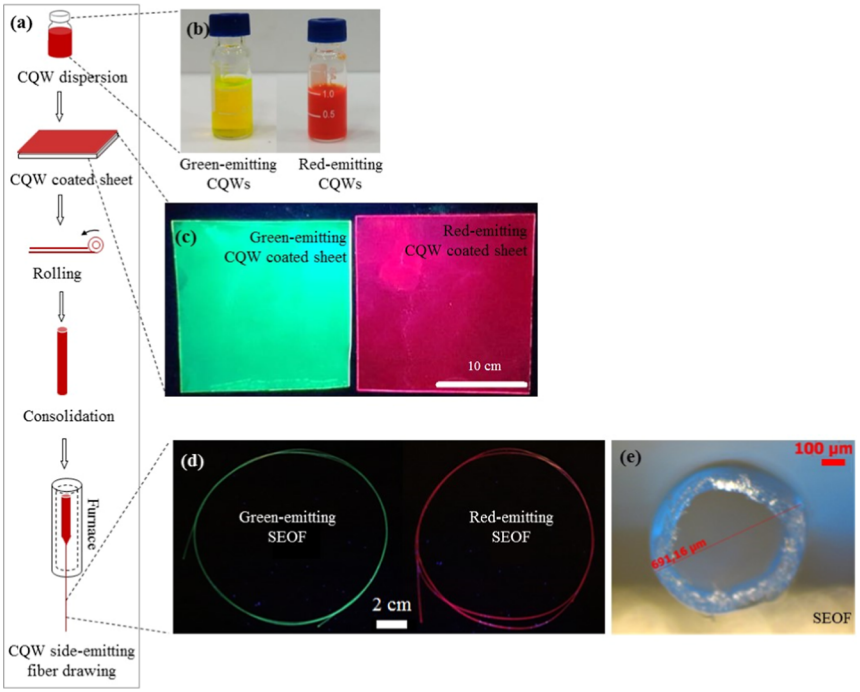

Figure 1. (a) Scheme illustrating the fiber fabrication process: CQW synthesis, PC sheet coating, rolling, consolidation, and fiber drawing. (b) Images of green- and red-emitting CQW dispersion. (c) Images of green- and red-emitting CQW-coated PC sheets under a UV lamp. (d) Images of green- and red-emitting CQW-doped SEOFs under a UV lamp and (e) microscopic cross-sectional image of the hollow-core SEOF.

limitations.[18,19] Colloidal quantum wells (CQWs) are a recent class of semiconductor nanocrystals that are considerably superior to other classes of luminescent nanocrystals, and to the best of our knowledge, there is no report on their usage in SEOFs. CQWs are multilayer semiconductor nanocrystals with thickness-dependent bandgaps, allowing for precise spectral tuning of the photoluminescence (PL). They offer greater flexibility in tuning the emission wavelength by controlling the size and composition of nanocrystals within their structure. This tunability is a significant advantage for specific applications, such as sensors and light sources.[20,21]

Different methods have been proposed so far for the integration of CQWs in optical fibers, including filling hollow-core fibers with a liquid containing nanocrystals[22,23] and coating the core of microstructured optical fibers[24,25] as postprocessing methods. These techniques are simple and flexible, but solvent evaporation and possible surface chemical reactions are the major drawbacks. Another method is the dispersion of CQWs in solid host material based on the polymerization process of the monomer. Two main challenges of this technique are the effect of initiator material on PL quenching and possible CQW aggregation.[21] On the other hand, 2-dimensional (2D) colloidal CQWs of group II−IV semiconductors, also known as nanoplatelets, possess extensive advantages over spherical quantum dots, which are critically necessary for the SEOF application. The CQWs exhibit a large absorption cross-section originating from their immense oscillator strength and anisotropic shape, which facilitates excitation below the band edge of the CQWs.[26] Moreover, the narrow PL full-width at half-maximum (fwhm) and high PL quantum yield (PLQY) ensure high color purity and efficiency of the SEOFs.

In this study, a novel method for CQW integration into hollow-core optical fibers for side-emitting applications is proposed and demonstrated. CQW nanoplatelets were utilized as the red- and green-emitting centers in the fibers. SEOFs were fabricated with different CQW concentrations by utilizing the coating of polymer sheets with nanoplatelets. Later, coated sheets were rolled to obtain a preform that was eventually transformed into a fiber via fiber drawing. The proposed method is simple and applicable, while there is no concern about the polymerization process or the surface chemical reactions. Optical characterization of CQWs and fabricated SEOFs was carried out including CQW absorption and PL spectra, scattering loss (SL), and diffusion length (DL) calculations.

EXPERIMENTAL SECTION

Chemicals. Cadmium acetate ($Cd(OAc)_2$, 99.995%), cadmium nitrate tetrahydrate ($Cd(NO_3)_2{\cdot}4H_2O$, ≥99.0%), cadmium acetate dihydrate ($Cd(OAc)_2 \times 2H_2O$, 98%), zinc acetate ($Zn(OAc)_2$, 99.99%), sodium myristate (≥99.0%), selenium (99.99%), sulfur (99.98%), 1-octadecene (ODE, 90%), 1-octanethiol (≥98.5%), oleic acid (OA, 90%), oleylamine (OLA, 70%), ethanol (absolute), *n*-hexane (≥97.0%), and methanol (≥99.7%) were obtained from Sigma-Aldrich.

Synthesis of 4 Monolayer CdSe Core CQWs. For the synthesis of 4 monolayer (ML) CdSe core CQWs, first, cadmium myristate was prepared via a standardized process.[27] In a typical synthesis, 800 mg of cadmium myristate, 67 mg of Se, and 60 mL of the ODE were mixed and degassed at 90 °C for 1 h. Then, the flask was flushed with Ar gas, the temperature was increased to 237.5 °C, and when the solution turned into golden yellow (at around 190−195 °C), 250 mg of $Cd(OAc)_2 \times 2H_2O$ was swiftly added to the flask. The solution was kept at 237.5 °C for 5 min, and then the flask was quenched in a water bath. The solution was collected, diluted with 25 mL of hexane, and centrifuged at 6000 rpm for 6 min. The supernatant was collected and the CQWs were separated from the unreacted chemicals and unwanted side-products through the addition of ethanol and centrifugation at 6000 rpm for 6 min. The precipitated CQWs were dissolved in hexane and kept for further use.

https://doi.org/10.1021/acsanm.4c06791
ACS Appl. Nano Mater. 2025, 8, 8603−8611

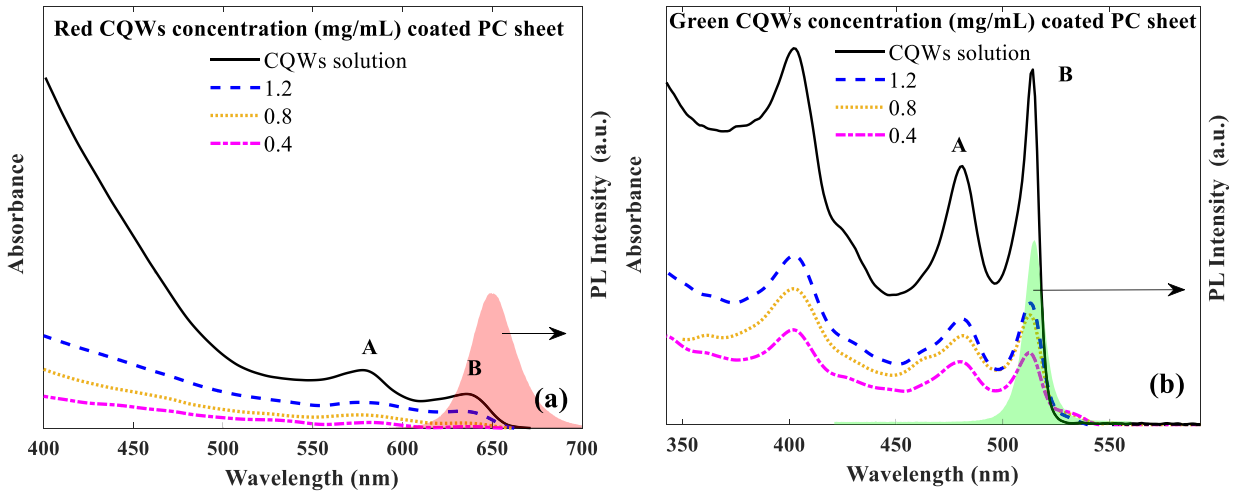

Figure 2. Absorbance and PL spectra of in-solution CQWs and different CQW concentration-coated PC sheets; (a) red-emitting CdSe/CdZnS core/shell CQWs and (b) green-emitting CdSe/CdS core/crown CQWs. Absorption peaks of A and B points correspond to E-HH and E-LH transitions, respectively.

Synthesis of 4 ML CdSe/CdS Core/Crown CQWs. The cation precursor was prepared by mixing 1.2 g of $Cd(OAc)_2 \times 2H_2O$, 0.85 mL of OA, and 5 mL of ODE at 100 °C.[28] The solution was consecutively sonicated and stirred at 100 °C to form a homogeneous white solution. In a typical synthesis, 8 mL of 4 ML CdSe core CQWs (with an optical density of one at the absorption wavelength of 350 nm, when 100 μL of the core solution was added to 3 mL of hexane), 700 mL of OA, and 10 mL of ODE were mixed in a 50 mL three-neck flask and vacuumed at room temperature for 1 h and further at 85 °C for 30 min to remove oxygen and other volatile species. Then, the flask was flushed with Ar gas, 4.8 mL of the cation precursor and 800 mL of S-ODE (0.1 M) were injected into the flask, and the temperature was increased to 225 °C. When the temperature reached 225 °C, the flask was quenched in a water bath and the core/crown CQWs were collected and diluted with hexane. The CQWs were precipitated through the addition of ethanol and centrifugation at 6000 rpm for 6 min and redispersed in hexane for further use.

Synthesis of CdSe/CdZnS Core/Shell CQWs. 8 mL of 4 ML CdSe core CQWs (with an optical density of one at the absorption wavelength of 350 nm, when 100 μL of the core solution was added to 3 mL of hexane), 0.6 mmol of $Zn(OAc)_2$, 0.2 mmol of $Cd(OAc)_2$, 2 mL of OA, and 8 mL of ODE were mixed in a 50 mL three-neck flask.[29] The solution was degassed at room temperature for 1 h and further at 85 °C for 30 min. Then, the flask was flushed with Ar gas, 2 mL of OLA was injected, and the temperature was adjusted to 300 °C. When the temperature reached 160 °C, an anion precursor of 1-octanethiol-ODE (0.1 M) was injected with an injection rate of 10 mL/h. The injection rate was decreased to 4 mL/h for temperatures above 240 °C. The injection was allowed to continue at 300 °C, while samples were taken to check the emission wavelength. When the desired emission wavelength was reached, the flask was quenched in a water bath, and the solution was diluted with 10 mL of hexane. The solution was centrifuged at 6000 rpm for 6 min to remove the colloidally unstable species, and then, the CQWs were precipitated from the supernatant through the addition of extra ethanol and centrifugation at 6000 rpm for 6 min. Finally, the CQWs were dissolved and kept in hexane.

Fabrication of CQW-Doped SEOFs. The five steps of the fabrication process of the SEOF are shown in Figure 1a. The first step, shown in Figure 1b, was the synthesis of CQWs in which the CdSe/CdZnS core/shell and CdSe/CdS core/crown were used for red and green emission, respectively, following the synthesis method described in the previous section. Based on the optical properties of polycarbonate (PC) in UV and visible range, coated PC sheets were prepared by dispersing different concentrations of CQWs over the two sides of the sheets. Samples with varying concentrations of 0.4, 0.8, and 1.2 mg/mL in hexane were prepared, and 20 × 20 cm^2 PC sheets were coated by a doctor blade coating tool for each concentration of red and green colors. Figure 1c shows the emission from red- and green-emitting CQW-coated sheets under a UV lamp. In the next step, six coated sheets were rolled on a metal guide rod and heated to 140 °C for 2 h and 185 °C for 50 min in vacuum. The consolidation process removes air gaps, adheres sheets to each other, completes the preform fabrication, and results in homogeneous dispersion of CQWs in PC. The final step was the fiber drawing in which a vertical furnace was heated up to 230 °C for uniform drawing of CQW-doped SEOFs with the help of a controllable motorized capstan and a preform feeder. The fabricated fibers have a hollow core with an outer diameter of 700 ± 10 μm as shown in Figure 1e.[30,31] The reflected light, including differential interference contrast in circularly polarized light (C-DIC), was utilized as a contrasting technique. The final fabricated SEOFs under the UV lamp are shown in Figure 1d, confirming the uniform emission of the nanoplatelets within the SEOF.

RESULTS AND DISCUSSION

CQW Absorption and PL Spectra. Starting with 4 ML CdSe core CQWs, green- and red-emitting CQWs were synthesized by employing different heterostructures based on the same core. The green CQWs were obtained by growing a lateral layer of the CdS crown around the core, which passivates the surface defects.[32] Growing the crown not only redshifts the PL peak wavelength by less than 5 nm (Figure S1a) but also enhances the PLQY substantially. For the red-emitting CQWs, an alloyed shell of CdZnS was grown in the vertical direction, which relaxes the quantum confinement. The PL spectrum (Figure S2b) can be tuned at longer wavelengths by controlling the size of the shell. Growing the shell not only enables spectral tuning but also enhances the PLQY by putting an inorganic passivating layer that prevents the electron and hole wave function distribution from reaching the surface of the CQWs.[33] Both sets of CQWs possess 2D morphologies, as shown in Figure S2, with average lateral sizes of 17.28 × 5.08 and 11.09 × 12.03 nm^2 for red and green CQWs, respectively. The X-ray diffraction pattern of green and red CQWs, shown in Figure S3, reveals zinc blende structure for both sets of NPLs with the diffracted peaks of red CQWs shifted to higher angles due to the smaller lattice constant of ZnS compared to CdS. Moreover, the XPS spectra of the participant elements in

https://doi.org/10.1021/acsanm.4c06791
ACS Appl. Nano Mater. 2025, 8, 8603−8611

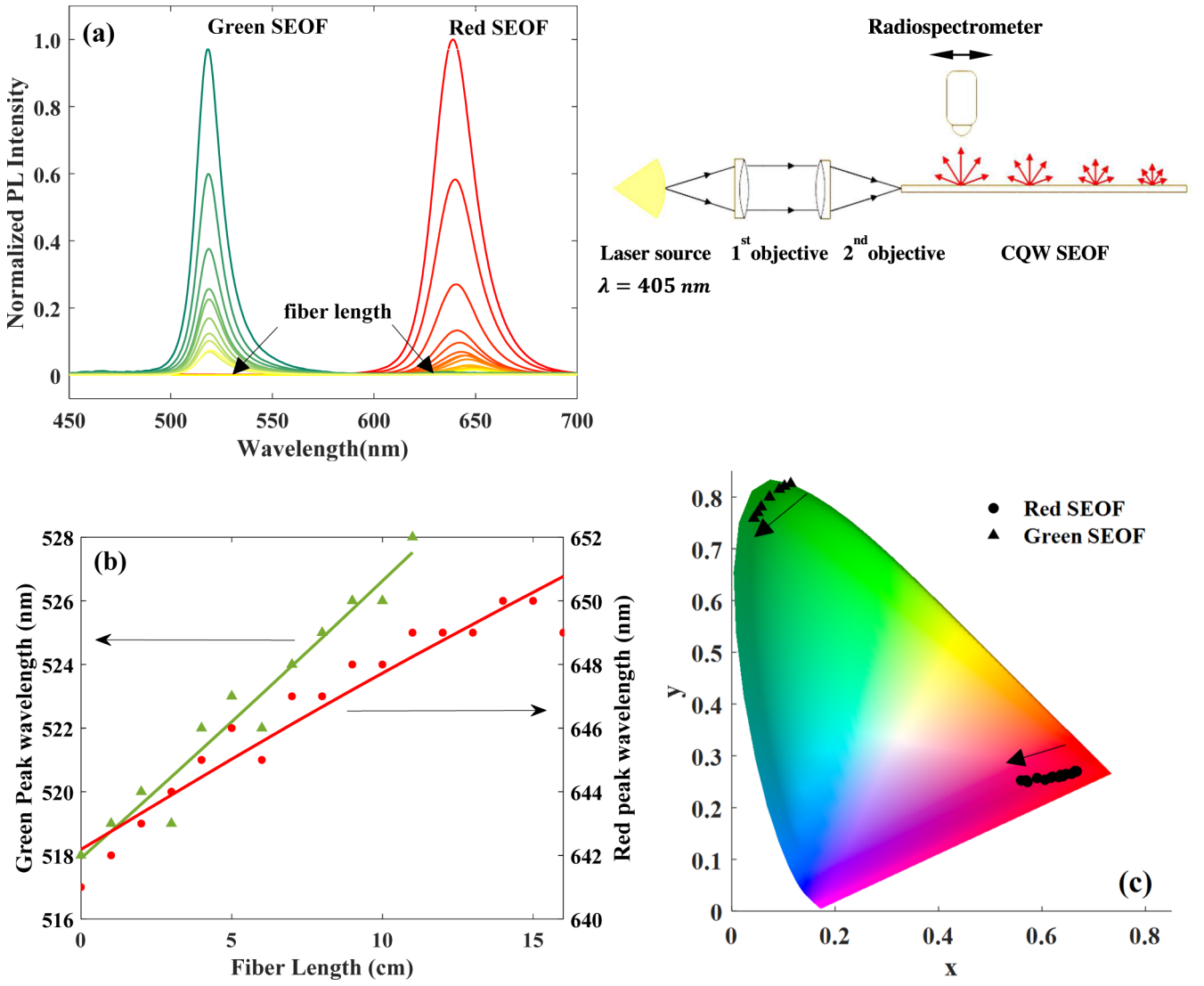

Figure 3. (a) Normalized scattered light intensity along every centimeter of the red and green SEOFs, which shows exponential decay, along with optical measurement setup for SL calculation of SEOFs. (b) PL peak red shift of scattered light along the fiber length for red and green SEOFs. (c) CIE diagram of scattered light while propagating in red and green SEOFs. The arrows show propagation through the fiber length.

green and red CQWs, shown in Figures S4 and S5, respectively, show successful formation of the crown or shell for the CQWs with no sign of oxidation of Se.

Absorbance and PL intensity spectra of red- and green-emitting CQWs are shown in Figure 2. Points A and B indicate the wavelengths in which the electron heavy-hole (E-HH) and electron light-hole (E-LH) transitions occur. These peaks are located at 580 and 641 nm for the red-emitting CQWs and 480 and 514 nm for the green-emitting ones. As shown with the shaded area, PL peaks are located at 650 and 515 nm for the corresponding CQWs. To investigate the effect of the PC surrounding area and the CQW concentrations, the absorbance of coated PC sheets at different concentrations was measured and is shown in Figure 2. The absorption peak wavelengths (A and B points) remained in their position while absorption increased with the concentration. For the red-emitting CQWs, at points A and B, the absorption reaches approximately 6% of CQW solution for a minimum intensity of 0.4 mg/mL, whereas it is around 26% for the green-emitting ones. Despite using same CQW concentrations, green absorption spectra appear more pronounced due to their higher absorption cross-section of the core/crown CQWs, which is associated with their larger lateral size.

The surrounding environment has a considerable impact on the optical characteristics of the CQWs. According to quantum electrodynamics and electromagnetics rules, the modes of propagation in optical fibers can influence the local density of optical states in the system.[35] This phenomenon can lead to changes in the decay rates, QY, and Purcell factor of the CQWs.[35] Hollow-core fibers support multimode propagation, with their cladding layer creating a semicavity that allows for multiple reflections. Given the overlap between the absorption and emission spectra of CQWs (as shown in Figure 2), the reabsorption within the optical fiber medium is expected to be greater than that of in solution. Moreover, an increase in CQW concentration leads to a higher reabsorption rate, which, in turn, decreases the QY. Additionally, the aggregation of CQWs into clusters is more likely to happen at higher concentrations, potentially affecting the performance of the CQWs.

The quantum yields for green and red CQWs are approximately 63.50% and 81.55%, respectively. Different parameters such as the polymeric environment, the potential

https://doi.org/10.1021/acsanm.4c06791
ACS Appl. Nano Mater. 2025, 8, 8603−8611

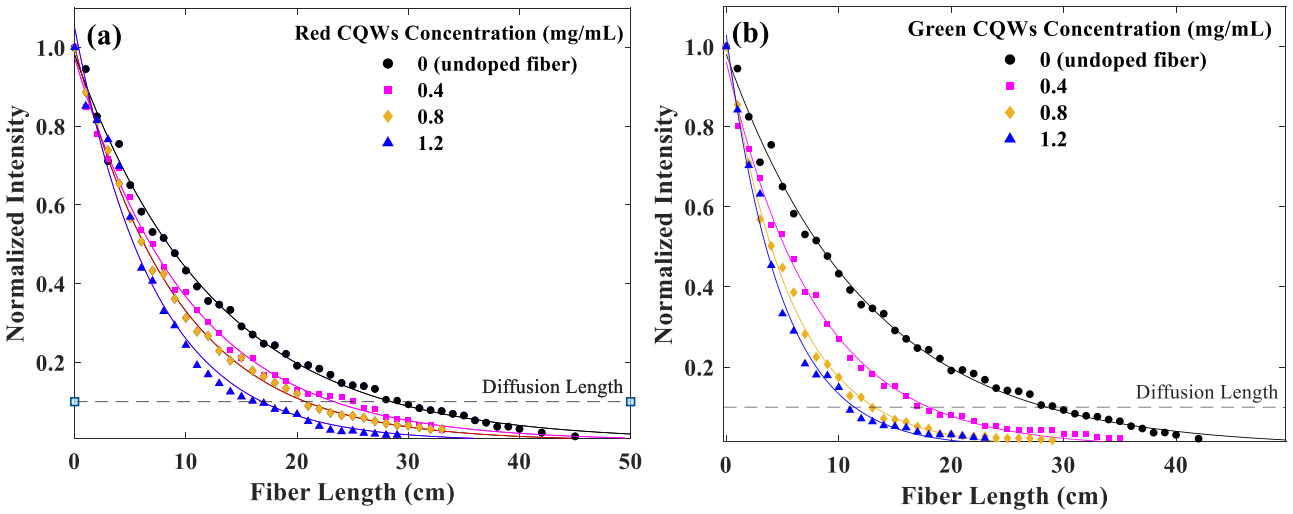

Figure 4. Normalized peak intensity of scattered light from undoped fiber and SEOFs using different CQW concentrations measured at every centimeter of the fibers: (a) red SEOF and (b) green SEOF. The points correspond to the measured peak intensity (Figure 3a) and the lines are exponential fitted curves.

for aggregation of CQWs, and the temperature conditions during the fiber drawing process contribute to a decrease in the QY. Our measurements for different concentrations of red and green CQWs indicate a relative QY value of 51 ± 5% and 34.4 ± 5% compared to the in-solution ones. The low loss of the fabricated fibers indicates the high potential of the method used in our work. We expect that using CQWs with higher PLQY, typically near unity,[36,37] would enhance the in-fiber PLQY and ultimately the performance of the final SEOF.

SEOF Optical Characterization. For the optical characterization of the fabricated SEOFs and their efficient light coupling, the measurement setup was aligned, as depicted in Figure 3a, which contains two objectives for collimating and focusing the input light. The distances between the laser source, objectives, and SEOF were calculated according to the laser spot size, objective characteristics, and optical fiber diameter. It is worth mentioning that connector-based coupling mechanism provides higher coupling efficiency and relatively a more uniform brightness distribution than our two-objective method as shown in Figure S1. Two input sources were used for our measurement: a supercontinuum laser source with output emission spanning between 450 and 2400 nm (YSL Photonics SC-5, China) and a 405 nm laser diode (DL5146-101S, THORLABS, USA) that was used for efficient excitation of CQWs. Figure 2 indicates a high absorption in 405 nm for both red- and green-emitting CQWs. Furthermore, the general behavior of SEOFs at different wavelengths was characterized while fibers were excited with the supercontinuum laser. The scattered light from SEOF was measured using a radio spectrometer typically positioned at every one-centimeter interval along the length of the fiber.

Figure 3a shows the scattered light intensity as a function of the length of green and red SEOFs suggesting that intensity decreases while propagating through the fiber. High and low decrement in the initial (<2 cm) and final lengths (>20 cm) of the fiber approve the exponential decay, which is depicted in Figure 4a,b for green- and red-doped fibers, respectively. Moreover, a red shift in the scattered peak wavelength is observed as illustrated in Figure 3b,c, which is associated with the polymer matrix surrounding the CQWs and reabsorption of light. Reabsorption is inevitable in CQWs due to their structure and electron transition bands, possibly reducing the structural efficiency.

CQW concentration in the polymer matrix is an important parameter that strongly affects the propagation length and SL of coupled light along the fiber. Generally, a higher concentration results in a higher SL and a shorter propagation length. Considering the exponential decay of light while propagating through the fiber, an exponential curve fitting was applied to the measured peak intensity of scattered light, and the SL value was calculated, accordingly. DL is defined as the distance in which the light intensity reaches 10% of its maximum value. The calculated SL and DL of different color-emitting SEOFs are shown in Table 1 according to measured data and fitted curves of Figure 4a,b. For better comparison, the SL and DL of bare fiber without CQWs were also calculated, which are 0.35 dB/cm and 29 cm, respectively. Hollow-core fibers have intrinsically high SL characteristics relative to solid-core fibers due to the low index air core medium. The DL of the bare structure can be considered as a baseline value that will be decreased by doping the CQWs. Different parameters can be used to control the decrement value, including CQW structure (CQW absorption and PL levels), CQW concentration, and fiber structure. In our study, the effect of CQW concentration was systematically investigated and is presented in Figure 4a,b. The reduction of DL in green SEOF is higher than that in the red one, probably due to the higher absorption cross-section of the green CQWs compared to the red CQWs, as discussed earlier. The higher

Table 1. Calculated SL and DL of Red and Green SEOFs with Different CQW Concentrations

CQW concentration (mg/mL)	red SEOF		green SEOF	
	SL (dB/cm)	DL (cm)	SL (dB/cm)	DL (cm)
0 (undoped fiber)	0.35	28.73	0.35	28.73
0.4	0.42	23.59	0.55	18.32
0.8	0.48	20.57	0.76	13.16
1.2	0.61	16.50	0.89	11.26

https://doi.org/10.1021/acsanm.4c06791
ACS Appl. Nano Mater. 2025, 8, 8603−8611

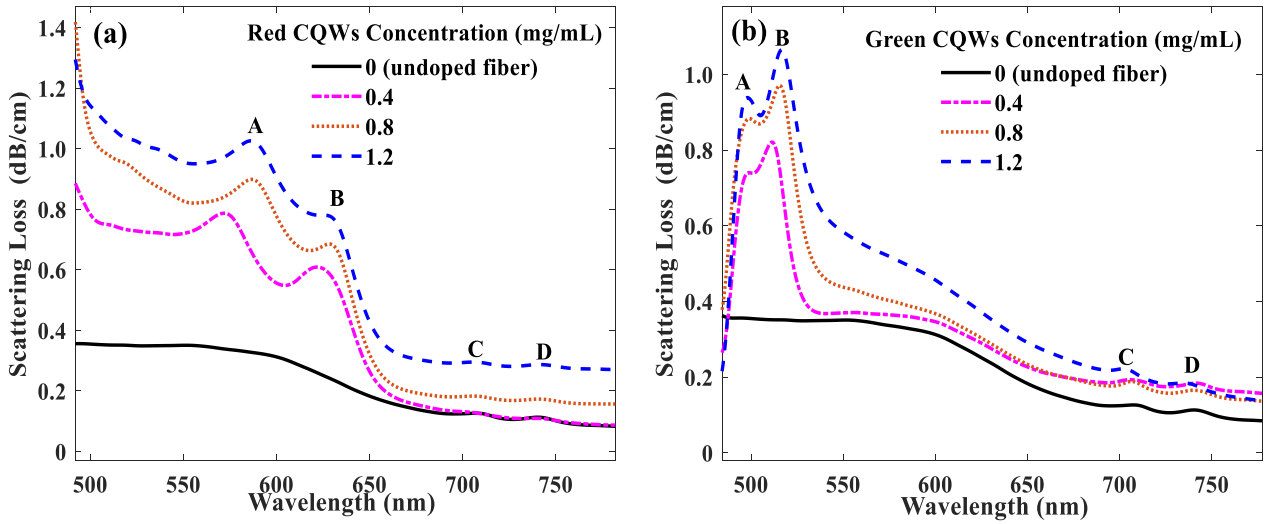

Figure 5. SL of undoped fiber and SEOFs with different CQW concentrations: (a) red SEOFs and (b) green SEOFs. Points A and B correspond to CQW E-HH and E-LH transitions, whereas points C and D correspond to C−H stretching overtone vibrations in PC.

Table 2. Comparison of the Reported Experiment with Our Proposed Method

integration method	fiber type	nanoparticle	application	$\lambda_{emission}$ (nm)	ref
polymerization	solid core	CdSe/CdS CQDs	light generating	525	21
polymerization	solid core	per and Rh6G	optical illuminator	441, 472, 503, 560	34
solution injection	holey fiber	CdSe/ZnS CQDs	light generation or amplification	594	35
solution injection	hollow core	PbSe	temperature sensor	1239, 1432	40
solution injection	hollow core	PbSe/CdSe CQDs	emission enhancement	997	22
sheet coating	hollow core	CdSe/CdS and CdSe/CdZnS CQWs	side emission	520, 640	this work

absorption cross-section implies a higher reabsorption of the emitted light, which intensifies the loss in the fiber. Moreover, as the Stokes shift decreases, the chance of reabsorption increases, compromising the fiber performance. The higher SL in the green SEOFs is partly due to the intrinsically higher absorption cross-section and lower Stokes shift of the green CQWs.

The cut-back method was used to investigate the spectral loss characteristics of SEOFs while the fibers were excited by the supercontinuum laser source. While propagating in the fiber, the input light coupled into the SEOF underwent absorption and emission by the CQWs. The main sources of absorption include the CQW dopants, fiber impurities, harmonics of molecular vibration, and carbon−hydrogen (C−H) stretching overtone bonds of a polymer medium. Among these, the CQWs absorb a large portion of incident light and isotropically emit at a longer wavelength. A considerable portion of the emitted light is scattered out of the fiber due to the hollow-core structure and unsatisfactory TIR condition. Moreover, fiber imperfections such as diameter variation, dust, bubbles, or scratches can also cause light scattering along with the Rayleigh and CQW scattering phenomena. In conventional optical fibers, minimizing the side scattering is an ideal point, while in SEOF, engineering and controlling the amount of scattered light is an objective. CQWs in our structure are intentionally added particles for side emission.

The black solid curve in Figure 5a,b shows the measured SL spectra of undoped fiber via the cut-back method in which a general decreasing trend is observed with two peaks, labeled as points C and D. The SL peaks labeled C and D in Figure 5, observed in the range of 700−750 nm, are attributed to the overtones or combination bands of C−H vibrations in the PC material. While such overtones are typically reported for polymers like PMMA and PS in the range of 700−800 nm,[21] the exact positions in PC differ due to its unique molecular structure, including aromatic groups and carbonate linkages. These assignments align with previously reported studies on near-infrared optical properties of PC fibers and films.[38,39] The same performance was observed in doped fibers, too. In the spectral regions $\lambda > 650$ nm and $\lambda > 530$ nm for red and green SEOFs, respectively, the dominant effect is the fiber hollow-core structure and PC host material. The increment of the SL value for the doped SEOF could be due to the possible cluster formation of CQWs and fabrication effects. In red SEOFs, for $\lambda < 650$ nm, absorption of CQWs dominates the spectral behavior. A sharp increase with two peaks, A and B, was observed, which was associated with the absorption spectra of red CQWs via E-HH and E-LH as depicted in Figure 2a. On the other hand, the green SEOF exhibited similar behavior as displayed in Figure 5b. In the spectral range $\lambda < 530$ nm, the absorbance of green CQWs is dominant (Figure 2b) with two peaks of points A and B which correspond to E-HH and E-LH, too. Regardless of the CQW absorbance characteristics, baseline SL of an undoped fiber is an essential factor that highly affects the overall SL level. The solid black lines in Figure 5a,b represent the baseline loss associated with polymeric material and fabrication variability. While this baseline may in principle vary between fiber samples depending on the manufacturing variation, as exemplified in Figure 5a,b, the absorption and scattering losses introduced by the CQWs are consistent and independent of fiber-to-fiber variation. These losses are additive to the intrinsic fiber loss, as demonstrated by the systematic measurements across multiple.

https://doi.org/10.1021/acsanm.4c06791
ACS Appl. Nano Mater. 2025, 8, 8603−8611

It is worth stating that simple hollow-core fibers exhibit high SL values. Integration of CQWs in nested hollow-core structures or solid-core fibers can further reduce the SL and consequently increase the DL.

In Table 2, a comparison of some reported experiments close to our work and our measurement is presented. It is worth noting that to the best of our knowledge, implementation of CQWs in optical fibers based on our proposed method is the first investigation focusing on a side-emitting application, which makes the comparison a bit challenging. As can be seen, our proposed method of fabrication is not as complex as polymerization nor as simple as solution injection, and it can easily cover the disadvantages of CQW quenching and instability of both methods. To further improve our proposed method's performance, it can be applied for solid core fibers in which the cladding part contains the coated sheets.

CONCLUSIONS

In this study, the integration of CQWs into a hollow-core optical fiber for side-emitting applications was developed and demonstrated for the first time. The synthesized red-emitting CdSe/CdZnS core/shell and green-emitting CdSe/CdS core/crown CQWs were incorporated into the cladding part of the hollow-core SEOF based on coating the polymer sheets with CQW solution. The measured scattered light confirms an exponential decay along the fiber length, which is in agreement with the SL values obtained by the cut-back method. The effect of CQW concentration on the SL value was understood, validating a higher value for a higher concentration rate. By controlling the size and composition, CQWs offer great flexibility in tuning absorption spectra and emission wavelength. This tunability can be considered as a critical point for the design of SEOFs for many specific applications, including medicine, healthcare monitoring, sensing, lighting, defense and security technologies, UV curing of resins and adhesives, and smart textiles.

ASSOCIATED CONTENT

Data Availability Statement

The data supporting this article have been included as a part of the paper. All data needed to evaluate the conclusions and results are present in the paper. Additional data related to this paper may be requested from the authors.

Supporting Information

The Supporting Information is available free of charge at https://pubs.acs.org/doi/10.1021/acsanm.4c06791.

CQWs and fiber characterization methods; optical characterization of the CQWs; and TEM images, XRD, and XPS measurements of the CQWs (PDF)

AUTHOR INFORMATION

Corresponding Author

Hilmi Volkan Demir − *Department of Electrical and Electronics Engineering, Department of Physics, UNAM-Institute of Materials Science and Nanotechnology and the National Nanotechnology Research Center, Bilkent University, Ankara 06800, Turkey; Luminous! Center of Excellence for Semiconductor Lighting and Displays, School of Electrical and Electronic Engineering, Division of Physics and Applied Physics, School of Physical and Mathematical Sciences, School of Materials Science and Engineering, Nanyang Technological University, Singapore 639798, Singapore;* orcid.org/0000-0003-1793-112X; Email: hvdemir@ntu.edu.sg, volkan@bilkent.edu.tr

Authors

Zahra Adelpour − *Department of Electrical and Electronics Engineering, Department of Physics, UNAM-Institute of Materials Science and Nanotechnology and the National Nanotechnology Research Center, Bilkent University, Ankara 06800, Turkey; Department of Electrical Engineering, Shiraz Branch, Islamic Azad University, Shiraz 7198774731, Iran*

Farzan Shabani − *Department of Electrical and Electronics Engineering, Department of Physics, UNAM-Institute of Materials Science and Nanotechnology and the National Nanotechnology Research Center, Bilkent University, Ankara 06800, Turkey;* orcid.org/0000-0003-2174-5960

Mojtaba Sadeghi − *Department of Electrical and Electronics Engineering, Department of Physics, UNAM-Institute of Materials Science and Nanotechnology and the National Nanotechnology Research Center, Bilkent University, Ankara 06800, Turkey; Department of Electrical Engineering, Shiraz Branch, Islamic Azad University, Shiraz 7198774731, Iran*

Aisan Khaligh − *Department of Electrical and Electronics Engineering, Department of Physics, UNAM-Institute of Materials Science and Nanotechnology and the National Nanotechnology Research Center, Bilkent University, Ankara 06800, Turkey;* orcid.org/0000-0002-5419-1020

Mahmudur Rahman − *UNAM-Institute of Materials Science and Nanotechnology and the National Nanotechnology Research Center, Bilkent University, Ankara 06800, Turkey*

Fırat Karaboğa − *Department of Electrical and Electronics Engineering, Department of Physics, UNAM-Institute of Materials Science and Nanotechnology and the National Nanotechnology Research Center, Bilkent University, Ankara 06800, Turkey; Department of Medical Services and Techniques, Mehmet Tanrikulu Vocational School of Health Services, Bolu Abant Izzet Baysal University, Bolu 14300, Turkey*

Emre Ünal − *Department of Electrical and Electronics Engineering, Department of Physics, UNAM-Institute of Materials Science and Nanotechnology and the National Nanotechnology Research Center, Bilkent University, Ankara 06800, Turkey;* orcid.org/0000-0002-8299-7435

Mustafa Ordu − *UNAM-Institute of Materials Science and Nanotechnology and the National Nanotechnology Research Center, Bilkent University, Ankara 06800, Turkey;* orcid.org/0000-0003-4049-9283

Complete contact information is available at: https://pubs.acs.org/10.1021/acsanm.4c06791

Author Contributions

The manuscript was written through contributions of all authors. All authors have given approval to the final version of the manuscript.

Notes

The authors declare no competing financial interest.

ACKNOWLEDGMENTS

The authors gratefully acknowledge the financial support from the Scientific and Technological Research Council of Türkiye (TUBITAK), Grant numbers 119N343, 121N395, and 20AG001. Z.A. and M.S. acknowledge the support from the Scientific and Technological Research Council of Türkiye

(TUBITAK-2221 program). H.V.D. also acknowledges the support from TUBA—Turkish Academy of Sciences.

REFERENCES

(1) Conneely, A. J.; Bennett, C.; O'Connor, G. M.; Vollmerhausen, T.; O'Byrne, C.; Spence, G.; Row, D.; Victor, J. Generation of Side-Emitting Polymer Optical Fibers by Laser Ablation for Use in Antimicrobial Applications. M604. In *International Congress on Applications of Lasers & Electro-Optics*, 2016; *1*

(2) Mordon, S.; Thécua, E.; Ziane, L.; Lecomte, F.; Deleporte, P.; Baert, G.; Vignion-Dewalle, A. S. Light Emitting Fabrics for Photodynamic Therapy: Technology, Experimental, and Clinical Applications. *Transl. Biophotonics* **2020**, *2* (3), No. e202000005.

(3) Živković, I.; Brajović, L.; Uskoković, P.; Aleksić, R. Indentation Damage Detection in Thermoplastic Composite Laminates by Using Embedded Optical Fibers. *J. Adv. Mater.* **2005**, *37* (1), 33−37.

(4) Bunge, C. A.; Kallweit, J. P.; Houri, M. A.; Mohr, B.; Berzios, A.; Grauberger, C.; Adi, P.; Gries, T. Textile Multitouch Force-Sensor Array Based on Circular and Non-Circular Polymer Optical Fibers. *IEEE Sens. J.* **2020**, *20* (14), 7548−7555.

(5) Lin, M. T. Quadri-Directional Optical Bending Sensor Using Side-Emitting POF Integrated with Wearable Device Technology in Smart Glove. *Int. J. Cloth. Sci. Technol.* **2022**, *34* (4), 502−515.

(6) Selm, B.; Gürel, E. A.; Rothmaier, M.; Rossi, R. M.; Scherer, L. J. Polymeric Optical Fiber Fabrics for Illumination and Sensorial Applications in Textiles. *J. Intell. Mater. Syst. Struct.* **2010**, *21* (11), 1061−1071.

(7) Kuhlmann, J. C.; Groeneveld, R.; Rees, H.; Timmerman, L.; Ebberink, G.; Timmermans, M.; Bottenberg, E.; Mahy, J. Smart Textile-Based Remote Identification System. In *Proceedings of the AUTEX 2019, 19th World Textile Conference on Textile at the Crossroads*; Ghent: Belgium, 2019, pp 11−15.

(8) Bier, S.; Mohr, B.; Marx, B.; Schiebahn, A.; Beckers, M.; Seide, G.; Bunge, C. A. Joining Intransparent Components by UV-Hardening Systems Through POF-Based UV-Light Initiation. In *Proceedings of the 25th International Conference on Plastic Optical Fibres*, 2016.

(9) Seewald, R.; Kallweit, J.; Weiland, J.; Schiebahn, A.; Gries, T.; Reisgen, U. Use of UV-Curing Adhesive Systems on Non-Transparent Joining Parts by Using Sidelight Activated Polymer Optical Fibres. In *In Industrial Applications of Adhesives*; Springer: Singapore, 2021; pp 1−14.

(10) Shah, M. A.; Pirzada, B. M.; Price, G.; Shibiru, A. L.; Qurashi, A. Applications of Nanotechnology in Smart Textile Industry: A Critical Review. *J. Adv. Res.* **2022**, *38*, 55−75.

(11) Pereira, C.; Pereira, A. M.; Freire, C.; Pinto, T. V.; Costa, R. S.; Teixeira, J. S. Nanoengineered Textiles: From Advanced Functional Nanomaterials to Groundbreaking High-Performance Clothing. In *Handbook of Functionalized Nanomaterials for Industrial Applications*; Elsevier, 2020; pp 611−714.

(12) Chen, J.; Zhan, Y.; Wang, Y.; Han, D.; Tao, B.; Luo, Z.; Ma, S.; Wang, Q.; Li, X.; Fan, L.; Li, C.; et al. Chitosan/Silk Fibroin Modified Nanofibrous Patches with Mesenchymal Stem Cells Prevent Heart Remodeling Post-Myocardial Infarction in Rats. *Acta Biomater.* **2018**, *80*, 154−168.

(13) Quandt, B. M.; Pfister, M. S.; Lübben, J. F.; Spano, F.; Rossi, R. M.; Bona, G. L.; Boesel, L. F. POF-Yarn Weaves: Controlling the Light Out-Coupling of Wearable Phototherapy Devices. *Biomed. Opt. Express* **2017**, *8* (10), 4316−4330.

(14) Wang, J.; Huang, B.; Yang, B. Effect of Weave Structure on the Side-Emitting Properties of Polymer Optical Fiber Jacquard Fabrics. *Textil. Res. J.* **2013**, *83* (11), 1170−1180.

(15) Shen, J.; Tao, X.; Ying, D.; Hui, C.; Wang, G. Light-Emitting Fabrics Integrated with Structured Polymer Optical Fibers Treated with an Infrared CO2 Laser. *Textil. Res. J.* **2013**, *83* (7), 730−739.

(16) Im, M. H.; Park, E. J.; Kim, C. H.; Lee, M. S. Modification of Plastic Optical Fiber for Side-Illumination. In *International Conference on Human-Computer Interaction*; Springer: Berlin, Heidelberg, 2007, pp 1123−1129.

(17) Křemenáková, D.; Militký, J.; Meryová, B.; Lédl, V. Characterization of Side Emitting Plastic Optical Fibers Light Intensity Loss. *World J. Eng.* **2013**, *10* (3), 223−228.

(18) Jakubowski, K.; Huang, C. S.; Boesel, L. F.; Hufenus, R.; Heuberger, M. Recent Advances in Photoluminescent Polymer Optical Fibers. *Curr. Opin. Solid State Mater. Sci.* **2021**, *25* (3), 100912.

(19) Schröder, J.; Reupert, A.; Wondraczek, L. Non-Resonant Luminescence Enhancement in Sol-Gel Coatings for Broadband UV-Light Conversion on Side-Emitting Optical Fibers. *Opt. Mater. Express* **2022**, *12* (6), 2318−2331.

(20) Kelestemur, Y.; Guzelturk, B.; Erdem, O.; Olutas, M.; Gungor, K.; Demir, H. V. Platelet-in-Box Colloidal Quantum Wells: CdSe/CdS@CdS Core/Crown@Shell Heteronanoplatelets. *Adv. Funct. Mater.* **2016**, *26* (21), 3570−3579.

(21) Whittaker, C. A.; Perret, A.; Fortier, C. W.; Tardif, O. M.; Lamarre, S. A.; Morency, S.; Larivière, D.; Beaulieu, L.; Messaddeq, Y.; Allen, C. N. Light-Generating CdSe/CdS Colloidal Quantum Dot-Doped Plastic Optical Fibers. *ACS Appl. Nano Mater.* **2020**, *3* (7), 6478−6488.

(22) Zhang, L.; Zhao, L.; Zheng, Y. Enhanced Emission from a PbSe/CdSe Core/Shell Quantum Dot-Doped Optical Fiber. *Opt. Mater. Express* **2018**, *8*, 3551−3560.

(23) Hreibi, A.; Gérôme, F.; Auguste, J.-L.; Dai, Q.; Yu, W. W.; Blondy, J.-M. PbSe Quantum Dots Liquid-Core Fiber. JTuD42. In *Conf. Lasers Electro-Optics*, 2010..

(24) DeHaven, S. L.; Williams, P. A.; Burke, E. R. Quantum Dots Microstructured Optical Fiber for X-Ray Detection. *AIP Conf. Proc.* **2015**, *1706*, 110012.

(25) Bravo, J.; Goicoechea, J.; Corres, J. M.; Arregui, F. J.; Matias, I. R. Encapsulated Quantum Dot Nanofilms Inside Hollow Core Optical Fibers for Temperature Measurement. *IEEE Sens. J.* **2008**, *8*, 1368−1374.

(26) Humayun, M. H.; Hernandez-Martinez, P. L.; Gheshlaghi, N.; Erdem, O.; Altintas, Y.; Shabani, F.; Demir, H. V. Near-Field Energy Transfer into Silicon Inversely Proportional to Distance Using Quasi-2D Colloidal Quantum Well Donors. *Small* **2021**, *17* (41), 2103524.

(27) Shabani, F.; Martinez, P. L. H.; Shermet, N.; Korkut, H.; Sarpkaya, I.; Dehghanpour Baruj, H.; Delikanli, S.; Isik, F.; Durmusoglu, E. G.; Demir, H. V. Gradient Type-II CdSe/CdSeTe/CdTe Core/Crown/Crown Heteronanoplatelets with Asymmetric Shape and Disproportional Excitonic Properties. *Small* **2023**, *19* (11), 2370072.

(28) Shabani, F.; Dehghanpour Baruj, H.; Yurdakul, I.; Delikanli, S.; Gheshlaghi, N.; Isik, F.; Liu, B.; Altintas, Y.; Canımkurbey, B.; Demir, H. V. Deep-Red-Emitting Colloidal Quantum Well Light-Emitting Diodes Enabled through a Complex Design of Core/Crown/Double Shell Heterostructure. *Small* **2022**, *18* (8), 2106115.

(29) Shabani, F.; Ahmad, M.; Kumar, S.; Delikanli, S.; Isik, F.; Bhattacharya, A.; Petrou, A.; Demir, H. V. Thermodynamic Silver Doping of Core/Shell Colloidal Quantum Wells Imparted with Paramagnetic Properties Emitting at Near-Infrared. *Chem. Mater.* **2023**, *35* (11), 4159−4170.

(30) Hasan, M. M.; Sadeque, M. S. B.; Albasar, I.; Pecenek, H.; Dokan, F. K.; Onses, M. S.; Ordu, M. Scalable Fabrication of MXene-PVDF Nanocomposite Triboelectric Fibers via Thermal Drawing. *Small* **2023**, *19* (6), 2206107.

(31) Rahman, M.; Ordu, M. Long-length 3D Printed Hollow-Core Polymer Optical Fiber for Wideband Light Guidance. *Opt. Fiber Technol.* **2023**, *81*, 103512.

(32) İzmir, M.; Sharma, A.; Shendre, S.; Durmusoglu, E. G.; Sharma, V. K.; Shabani, F.; Baruj, H. D.; Delikanli, S.; Sharma, M.; Demir, H. V. Blue-Emitting CdSe Nanoplatelets Enabled by Sulfur-Alloyed Heterostructures for Light-Emitting Diodes with Low Turn-On Voltage. *ACS Appl. Nano Mater.* **2022**, *5* (1), 1367−1376.

(33) Baruj, H. D.; Bozkaya, I.; Canimkurbey, B.; Isik, A. T.; Shabani, F.; Delikanli, S.; Shendre, S.; Erdem, O.; Isik, F.; Demir, H. V. Highly-Directional, Highly-Efficient Solution-Processed Light-Emitting Di-

https://doi.org/10.1021/acsanm.4c06791
ACS Appl. Nano Mater. 2025, 8, 8603−8611

odes of All-Face-Down Oriented Colloidal Quantum Well Self-Assembly. *Small* **2023**, *19* (29), 2206582.
(34) Miluski, P.; Dorosz, D.; Kochanowicz, M.; Żmojda, J. Fluorescent Polymeric Optical Fibre Illuminator. *Electron. Lett.* **2016**, *52* (18), 1550−1552.
(35) Meissner, K. E.; Holton, C.; Spillman, W. B., Jr. Optical Characterization of Quantum Dots Entrained in Microstructured Optical Fibers. *Phys. E* **2005**, *26* (1−4), 377−381.
(36) Zhu, Y.; Deng, Y.; Bai, P.; Wu, X.; Yao, Y.; Liu, Q.; Qiu, J.; Hu, A.; Tang, Z.; Yu, W.; Li, Y.; Jiang, P.; Liu, Z.; Gao, P.; Hao, Y.; et al. Highly Efficient Light-Emitting Diodes Based on Self-Assembled Colloidal Quantum Wells. *Adv. Mater.* **2023**, *35* (49), 2305382.
(37) Hu, A.; Bai, P.; Zhu, Y.; Song, Z.; Wang, R.; Zheng, J.; Yao, Y.; Zhang, Q.; Ding, Z.; Gao, P.; Sui, X.; et al. Green CdSe/CdSeS Core/Alloyed-Crown Nanoplatelets Achieve Unity Photoluminescence Quantum Yield over a Broad Emission Range. *Adv. Opt. Mater.* **2022**, *10* (13), 2200469.
(38) Groh, W. Overtone Absorption in Macromolecules for Polymer Optical Fibers. Die Makromol. Chem. *Macromol. Chem. Phys.* **1988**, *189* (12), 2861−2874.
(39) Tomoyoshi Yamashita, T. Y.; Kensuke Kamada, K. K. Intrinsic Transmission Loss of Polycarbonate Core Optical Fiber. *Jpn. J. Appl. Phys.* **1993**, *32* (6R), 2681.
(40) Zhang, Z.; Wang, Y.; Jiang, Y.; Feng, Y.; Wang, H.; Zhang, T.; Zhuang, X.; Zhang, J.; Ma, Y.; Xing, X.; Yu, S.; et al. Colloidal PbSe Quantum Dot-Filled Liquid-Core Optical Fiber for Temperature Sensing. *Mater. Res. Express* **2019**, *6* (7), 075040.

https://doi.org/10.1021/acsanm.4c06791
ACS Appl. Nano Mater. 2025, 8, 8603−8611